Photoinduced Phase Transition of Azobenzene-Coupled Benzenetricarboxamide

Yashwardhan R. Malpani,[†,‡] Seungwhan Oh,[§] Sumi Lee,[§] Young-Sik Jung,[†,‡,*] and Jong-Man Kim[§,#,*]

[†]*Division of Drug Discovery Research, Korea Research Institute of Chemical Technology, P.O. Box 107, Yuseong,*
*Daejeon 305-600, Korea. *E-mail: ysjung@krict.re.kr*
[‡]*Department of Medicinal and Pharmaceutical Chemistry, University of Science and Technology, Daejeon 305-355, Korea*
[§]*Department of Chemical Engineering, Hanyang University, Seoul 133-791, Korea. *E-mail: jmk@hanyang.ac.kr*
[#]*Institute of Nano Science and Technology, Hanyang University, Seoul 133-791, Korea*

1,3,5-Benzenetricarboxamide (BTC) family have been actively explored as supramolecular scaffolds especially for columnar structures.[1-12] It is well known that in BTC derivatives the presence of three amide groups that can participate in strong three-fold intermolecular hydrogen bonding and the planar aromatic core could assist in better columnar packing through π-π stacking interactions. Addition of functional groups to BTC derivatives makes these supramolecular scaffolds more intriguing. For instance, we reported a thermosensitive BTC system by introduction of hydrophilic crown ether moieties to the BTC core.[13] The crown ether containing BTC displayed a lower critical solution temperature (LCST) behavior owing to the thermosensitive crown ether groups. More recently, we described a photoresponsive BTC, Azo-BTC, that is derived from an azobenzene chromophore (Figure 1).[14]

It was observed that the azobenzene containing Azo-BTC forms strikingly different morphologies based on the condition employed for the self-assembly of these supramolecules. These supramolecules forms fibers, gels and hollow spheres based on the solvent used for the self-assembly. Especially, in contrast to the fibrous Azo-BTC supramolecules formed in aqueous DMSO and DMF solutions, nano/microsized spheres are generated from self-assembly of Azo-BTC in a

mixture of THF and water which are composed of a mixture of bulk and hollow spheres. It was also observed that a reversible photo-induced phase transition occurred on irradiation with UV (330-385 nm) and visible light (460-490) with these fibers.

Bromine is a bulky atom as well as it is known to imparts lipophilic character to the hydrocarbons like other halogens[15-17] and thus alter solubility and polarity of a compound. With our earlier experience that the solubility and structure of Azo-BTC have effect on its morphology and phase transition character in different self-assembly conditions, we were interested to know the effects of bromo substitution as in Br-Azo-BTC.

During the course of studies aimed at the development of one-dimensional nanostructures using BTC derivatives, we observed that the azobenzene-containing BTC, N^1,N^3,N^5-tris(4-((E)-(4-bromophenyl)diazenyl)phenyl)benzene-1,3,5-tricarboxamide (Br-Azo-BTC) (Figure 1) displays photoinduced phase transitions in aqueous DMF and THF. Unlike Azo-BTC, the bromosubstituted Br-Azo-BTC shows different morphologies and phase transition behaviors.

The synthesis of Br-Azo-BTC was accomplished efficiently in high yields (Scheme 1). 4-Bromoaniline was oxidized to its nitroso derivative using oxone. The bromonitrosobenzene was coupled with 1,4-phenylene diamine under anhydrous conditions to a gives the desired bromosubstituted azobenzene.[18] Then usual amide formation protocol with 1,3,5 benzene tricarbonyl trichloride and amine in the presence of
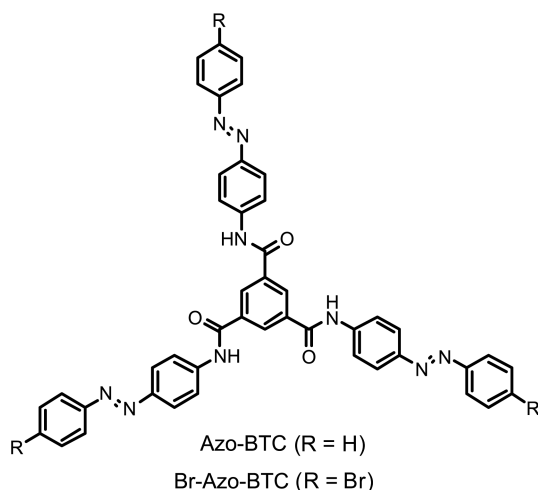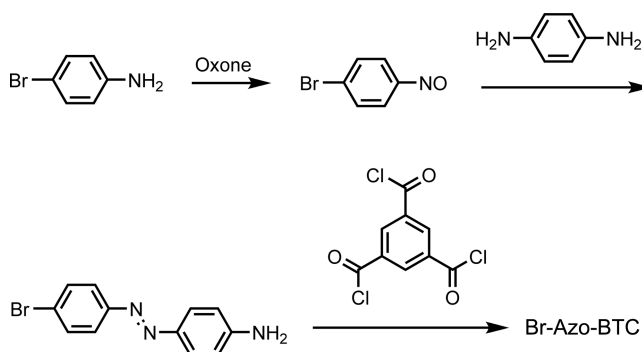

Figure 1. Structure of Azo-BTC and Br-Azo-BTC.

Scheme 1. Preparation of Br-Azo-BTC.

triethylamine gave the desired Br-Azo-BTC. The structure of the Br-Azo-BTC was confirmed by ^{1}H-NMR, ^{13}C-NMR and HRMS analysis of the compound.

The bromo azobenzene containing BTC, Br-Azo-BTC is soluble in organic solvents, such as dimethylsulfoxide (DMSO), *N,N*-dimethylformamide (DMF), and tetrahydrofuran (THF). Addition of water to a solution containing Br-Azo-BTC (10 mM), results in self-assembly of these supramolecules in nano-micro structures. Based on the fact that the dielectric medium of the solvents has a huge effect on the formation of fibers and sphere,[14] we expected different morphologies in case of Br-Azo-BTC with different solvents. Indeed, these aggregates also shows different morphologies based on the self-assembly conditions employed. But surprisingly, in contrast to the fibers obtained in DMSO in Azo-BTC, the Br-Azo-BTC in 50% DMSO-H_2O aggregates doesn't shows a distinct morphology, instead amorphous aggregation of these supramolecules was observed (data not shown). Interestingly, the Br-Azo-BTC in 50% DMF-H_2O self-assembles into fine micro fibers (Figure 2(a), left). Irradiation of UV light (330-385 nm) for 10 s results in disappearance of the fibrous Br-Azo-BTC supramolecules (Figure 2(b), left). Regeneration of the fibers takes place when the UV-treated sample is exposed to visible light (460-490 nm) for 5 min (Figure 2(c), left). UV light irradiation of the regenerated fibers causes melting of the supramolecules. These light-induced phase transitions of Br-Azo-BTC supramolecules can be repeated numerous times without decomposition of the material.

Unlike Azo-BTC that forms hollow/bulk spheres in aqueous THF, Br-Azo-BTC is found to yield microfibers in 50% THF-H_2O (Figure 2(a), right). The formation of fiber morphology in aqueous THF with Br-Azo-BTC in contrast to Azo-BTC is presumably due to the higher solubility of the Br-Azo-BTC in THF compared to Azo-BTC. Thus, when water is added to a solution of Br-Azo-BTC in THF it feels less abrupt change in solvent nature due to being more solubilized in THF. Thus, it slowly separates out from the solvent system with gradual hydrogen bond formation between the supramolecules and thus results in a uniform fiber growth. Moreover the microfibers obtained in aqueous THF were thinner and flexible compared to those obtained in aqueous DMF. This may be due to the lesser solvent assisted hydrogen bonding in aqueous THF condition, as only water molecules are available for solvent assisted hydrogen bonding. Thus stacking of these supramolecules is not much promoted. But, in case of aqueous DMF systems there are extra DMF molecules which are present in large portion to assist in thicker growth of the fibers which may promote the stacking arrangement.

UV light treatment of the microfibers obtained in aqueous THF resulted in the phase separation phenomenon (Figure 2(b), right). It is expected that the Br-Azo-BTC's *cis*-form is much polar to get homogenously dissolved in aqueous THF and thus they are phased out from the solvent system. Irradiation of visible light to the phase separated supramolecules in aqueous THF allowed regeneration of fibers (Figure 2(c),
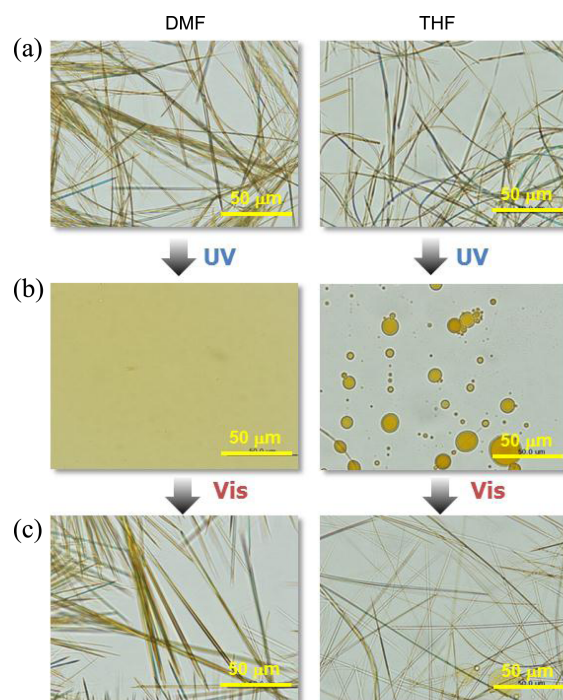

Figure 2. (a) Optical microscope images of the Br-Azo-BTC supramolecules prepared in 50% DMF-H_2O (left) and in 50% THF-H_2O (right). (b, c) Optical microscopic images upon UV (b) and visible (c) light irradiation.

right). The remarkable point is that, the microfiber regeneration process occurs only unidirectional and after a certain "cut-off width" of these micro-fibers, further growth of the fibers takes place only longitudinally.

Experiments were carried out to probe the effect of the three amide groups present in Br-Azo-BTC on the supramolecular architectures and the observed morphological change. It is well known that fluoride anion is a sufficiently strong base to abstract imide or amide protons in conjugated molecules.[19] Amide proton abstraction by fluoride often results in significant changes in the electronic absorption and emission properties of the conjugated molecules. If fluoride anion abstracts protons from the amide groups in the Br-Azo-BTC supramolecules, detectable morphological changes are expected. In order to test this proposal, tetrabutylammonium halides (F, Cl, Br, I, 20 molar equivalent) were added to DMF solutions containing Br-Azo-BTC. As displayed in Figure 3(a), the vial exposed to fluoride anion becomes wine-red while to vials not exposed to anions (control) or exposed to other anions (Cl, Br, I) retain the original orange-yellow color associated with the azo chromophore. Further addition of water does not generate any fibers in case of vial containing fluoride anion but fibers were formed as usual in case of vials containing other anions. In addition, an aqueous DMF solution containing Br-Azo-BTC supramolecules became clear upon exposure to fluoride anion (Figure 3(b)). Images observed by using optical microscopy reveal that complete disappearance of the fiber morphology takes place when these fibers were exposed to fluoride anion (data not shown). These results demonstrate that fluoride anion is
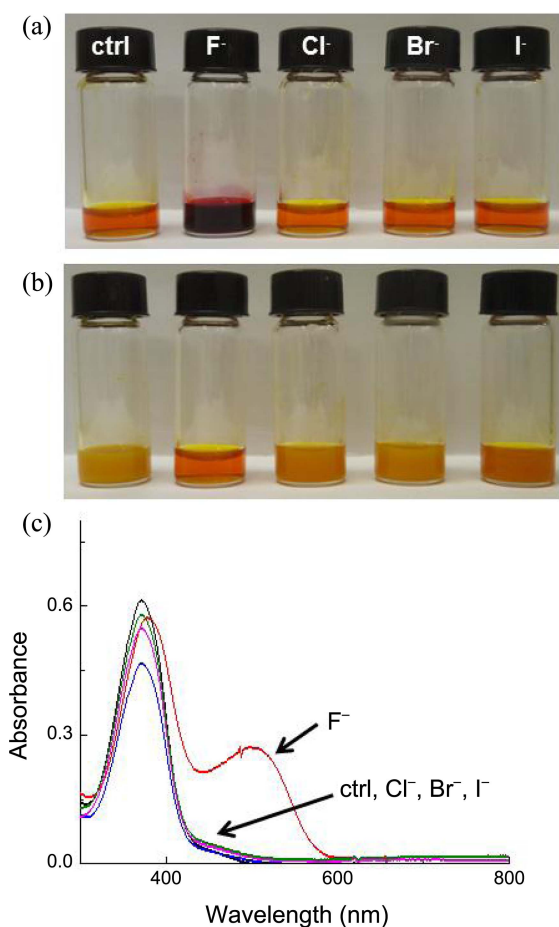
(a)

(b)

(c)

Figure 3. (a) Vials containing Br-Azo-BTC in DMF in the presence of anions. (b) Vials containing Br-Azo-BTC fibers in 50% DMF-H$_2$O upon exposure to anions. (c) UV-Vis spectra of Br-Azo-BTC fibers in 50% DMF-H$_2$O upon exposure to anions.

capable of destroying the aggregates of Br-Azo-BTC supramolecules. Inspection of the effect of fluoride anion on the Br-Azo-BTC supramolecules by utilizing UV−Vis spectroscopy reveals that the presence of fluoride anion results in the appearance of a new absorption maximum at 520-530 nm, which is responsible for the wine-red color generation (Figure 3(c)). This clearly indicates the change in the conjugated form of the Br-Azo-BTC. This results shows that the amide bond are crucial in case of Br-Azo-BTC to form the fibrous self-assembled structures as reported earlier for Azo-BTC.[14]

With our previous experience and based on the above observations, it is clear that formation of distinct morphologies under self-assembly conditions is not only dependent on the solvent medium but also on the structure of the supramolecule. In fact, physical properties of compounds are known to alter with the changes in structural and dipolar nature of the compounds. Thus a change in dipolar nature of cis and trans form of Azo-BTC which is seen in Br-Azo-BTC can results in difference in the solubility of cis and trans form of the compounds in different solvent, which in turn can also affect the rate of self-assembly, giving distinct and varied morphologies. Importantly, a sudden difference

in the solvent medium results in the abrupt amorphous aggregation of these compounds but a uniform and slow growth, which could be result of appropriate change of the solvent polarity, must results in the formation of distinct morphologies as seen by optical microscopic images. Thus, Br-Azo-BTC does not results in self-assembled structures in aqueous DMSO medium. In contrast, we were able to obtain nicely grown microfibers in aqueous DMF and in aqueous THF.

In conclusion, microfibers from self-assembly of an azobenzene containing BTC derivative, Br-Azo-BTC, were obtained in different self-assembly conditions. The Br-Azo-BTC forms differently sized fibers in DMF/H$_2$O and THF/H$_2$O conditions. These fibers obtained in DMF/H$_2$O and THF/H$_2$O shows reversible phase transitions upon alternating UV and visible light irradiation. The reversible morphological transition is due to the photoinduced *cis-trans* isomerism in azobenzene units. Interestingly, the fibers growth takes place selectively in longitudinally fashion which is more prominent in THF/H$_2$O conditions giving very thin microfibers. The exact nature of this longitudinal growth is still under study but role of solvent is supposed to play an important role in the formation of hydrogen bond at the amide functionality during regeneration of fibers. Most probably due to solvent assisted/mediated hydrogen bonding. The nature of solvent has huge role to play in this effect which shows that the solvent molecules may involve in the H-bond formation between the stacked molecules.

Experimental

Materials and Instruments. Unless otherwise stated, all commercially available solvents and reagents were used without further purification. Melting points were recorded on Mettler Toledo MP50 apparatus and are uncorrected. IR spectra were recorded on an FT-IR Smiths Identify IR and the values are mentioned in cm^{-1}. The ^{1}H-NMR and ^{13}C-NMR was recorded on Varian and Bruker NMR spectrophotometer, using commercial NMR solvents obtained from Aldrich with TMS as internal standard and chemical shifts are mentioned in δ ppm scale. The Mass spectra were obtained over Varian 1200L quadrupole MS (EI) spectrophotometer.

4-Bromophenylazoaniline (C$_{12}$H$_{10}$BrN$_3$). To a dichloromethane solution (50 mL) containing para-bromoaniline (2.50 g, 14.5 mmol) was added oxone (17.86 g, 29.0 mmol) in water (150 mL). The mixture was kept at room temperature for 4 h and then layers were separated. The aqueous layer was extracted with dichloromethane (100 mL × 3). Combined organic layer was washed with dil. HCl (1 N, 100 mL), sat. NaHCO$_3$ (100 mL), water (100 mL) and brine (100 mL). Drying over anhydrous sodium sulfate was followed by concentration to yield the crude nitroso intermediate (quant.). The crude was then dissolved in glacial AcOH (40 mL) immediately and to this solution was added 1,4-phenylenediamine (1.57 g, 14.5 mmol) in dry DMSO (10 mL). The resultant mixture was stirred at room temperature for two

days and then concentrated to remove acetic acid. This crude was taken up in brine (500 mL) and extracted with ethyl acetate (150 mL × 5). The combined organic layer was washed with 10% NaCl solution (100 mL × 2), dried over anhydrous sodium sulfate, and concentrated to give the crude mass which was purified over silica gel column chromatography (20% EA in hexanes) to yield the pure product as brown solid. Yield: 2.40 g (60%); mp 112-115 $^{\circ}$C; ^{1}H-NMR (300 MHz, CDCl$_3$) δ 4.09 (br, 2H, NH$_2$), 6.74 (d, J = 8.7 Hz, 2H, ArH), 7.60 (d, J = 8.7 Hz, 2H, ArH), 7.72 (d, J = 8.7 Hz, 2H, ArH), 7.80 (d, J = 8.7 Hz, 2H, ArH). HRMS (EI): calculated 275.0058, found 275.0049. IR (neat): 3400, 1625, 1594, 1572, 1461, 1302, 1137, 1066, 1002, 826, 737 cm^{-1}.

N^1,N^3,N^5-Tris(4-((E)-(4-bromophenyl)diazenyl)phenyl) benzene-1,3,5-tricarboxamide (C$_{45}$H$_{30}$Br$_3$N$_9$O$_3$). To a solution of benzene-1,3,5-tricarbonyl trichloride (1.00 g, 3.8 mmol) in dry THF (40 mL) was added triethylamine (3.15 mL, 22.6 mmol) and 4-bromophenylazoaniline (3.44 g, 12.4 mmol). The resulting mixture was stirred under a reflux condition for 2 days. The precipitates formed were removed and the filtrate was concentrated *in vacuo*. The residue was re-dissolved in THF and slowly precipitated with large excess of MeOH. The precipitate obtained was filtered off and washed with MeOH (50 mL) and dichloromethane (20 mL) to yield the product as yellow powder. Yield: 3.70 g (95%); mp > 300 $^{\circ}$C. ^{1}H-NMR (300 MHz, DMSO-d_6) δ 7.79-7.86 (m, 12H, ArH), 8.00 (d, J = 9.0 Hz, 6H, ArH), 8.12 (d, J = 9.0 Hz, 6H, ArH), 8.18 (s, 3H, ArH), 11.06 (s, 3H, NH); ^{13}C-NMR (temp. 90 $^{\circ}$C, 125 MHz, DMSO-d_6) δ 120.4, 123.0, 123.6, 123.7, 129.5, 131.9, 135.0, 141.7, 148.0, 150.9, 164.3. HRMS (ESI): calculated 979.9943 (M $-$ H$^+$), found 979.9895 (M $-$ H$^+$). IR (neat): 3375, 3085, 1671, 1594, 1525, 1500, 1404, 1304, 1247, 1151, 1065, 1005, 837, 727 cm^{-1}.

References

1. Cantekin, S.; de Greef, T. F. A.; Palmans, A. R. A. *Chem. Soc. Rev.* **2012**, *41*, 6125-6137.
2. Stals, P. J. M.; Haveman, J. F.; Palmans, A. R. A.; Schenning, A. P. H. J. *J. Chem. Educ.* **2009**, *86*, 230-233.
3. Roosma, J.; Mes, T.; Leclere, P.; Palmans, A. R. A.; Meijer, E. W. *J. Am. Chem. Soc.* **2008**, *130*, 1120-1121.
4. van Gorp, J. J.; Vekemans, J. A. J. M.; Meijer, E. W. *J. Am. Chem. Soc.* **2002**, *124*, 14759-14769.
5. Bose, P. P.; Drew, M. G. B.; Das, A. K.; Banerjee, A. *Chem. Commun.* **2006**, 3196-3198.
6. Shikata, T.; Ogata, D.; Hanabusa, K. *J. Phys. Chem. B* **2004**, *108*, 508-514.
7. Ryu, S. Y.; Kim, S.; Seo, J.; Kim, Y.-W.; Kwon, O.-H.; Jang, D.-J.; Park, S. Y. *Chem. Commun.* **2004**, 70-71.
8. Lee, S. J.; Park, C. R.; Chang, J. Y. *Langmuir* **2004**, *20*, 9513-9519.
9. Lewis, F. D.; Long, T. M.; Stern, C. L.; Liu, W. *J. Phys. Chem. A* **2003**, *107*, 3254-3262.
10. Lightfoot, M. P.; Mair, F. S.; Pritchard, R. G.; Warren, J. E. *Chem. Commun.* **1999**, 1945-1946.
11. Paraschiv, I.; Giesbers, M.; van Lagen, B.; Grozema, F. C.; Abellon, R. D.; Siebbeles, L. D. A.; Marcelis, A. T. M.; Zuilhof, H.; Sudholter, E. J. R. *Chem. Matter.* **2006**, *18*, 968-974.
12. Masuda, M.; Jonkheijm, P.; Sijbesma, R. P.; Meijer, E. W. *J. Am. Chem. Soc.* **2003**, *125*, 15935-15940.
13. Lee, S.; Lee, J. S.; Lee, C. H.; Jung, Y. S.; Kim, J. M. *Langmuir* **2011**, *27*, 1560-1564.
14. Lee, S.; Oh, S.; Lee, J.; Malpani, Y.; Jung, Y. S.; Kang, B.; Lee, J. Y.; Ozasa, K.; Isoshima, T.; Lee, S. Y.; Hara, M.; Hashizume, D.; Kim, J. M. *Langmuir* **2013**, *29*, 5869-5877.
15. Dorwald, F. Z. *Lead Optimization for Medicinal Chemists*; Strauss GmbH: Morlenbach, 2012; pp 49-57.
16. Pliska, V., Testa, B., van de Waterbeemd, H., Eds.; *Lipophilicity in Drug Action and Toxicology* (*Methods and Principles in Medicinal Chemistry*; Vol. 4); VCH: Weinheim, New York, Basel, Cambridge, Tokyo, 1996.
17. Thomas, G. *Medicinal Chemistry an Introduction*, 2nd ed.; John Wiley & Sons: West Sussex, UK, 2000.
18. Priewisch, B.; Ruck-Braun, K. *J. Org. Chem.* **2005**, *70*, 2350-2352.
19. Qu, Y.; Hua, J.; Tian, H. *Org. Lett.* **2010**, *12*, 3320-3323.